NEW FRICTION FACTOR AND HEAT TRANSFER COEFFICIENT EQUATIONS FOR LAMINAR FORCED CONVECTION OF LIQUID WITH VARIABLE PROPERTIES IN STRAIGHT TUBES

Houjian Zhao, Xiaowei Li*, Xinxin Wu
*Author for correspondence
Institute of Nuclear and New Energy Technology,
Tsinghua University,
Beijing 100084,
China,
E-mail: lixiaowei@tsinghua.edu.cn

ABSTRACT

When there are large temperature differences between the wall and the fluid, the friction factors and heat transfer coefficients of forced laminar convection with variable fluid properties are different from the theoretical results deduced with constant property assumptions. However, most existing equations for variable properties are obtained by regression analysis of experimental data with a specific kind of fluid, and cannot reflect the property-temperature sensitivities at different fluid temperatures and for different kinds of liquid. In this paper, the governing equations of forced laminar convection of ethanol and water are numerically solved using CFD method and the results are used to verify the deduced equations. Compared with dynamic viscosity, the variations of density, thermal conductivity and specific heat capacity in the cross section can be neglected. A new explicit equation of friction factor and a new explicit equation of heat transfer coefficient for forced liquid laminar convection with variable properties heated in straight tubes are obtained. The deduced equations show good predictions of friction factors and Nusselt numbers for different kinds of liquid. Based on the equations, a dimensionless parameter is derived to predict the heat flux effects and viscosity-temperature sensitivities on friction factors and heat transfer coefficients.

INTRODUCTION

Conventional friction factor and heat transfer coefficient equations of laminar flow in straight tubes are deduced on the basis of constant property assumptions. However, when the temperature difference, $\Delta T = T_w - T_b$, is large, the properties show large variations in the cross section. Equations deduced from constant property assumption will deviate largely from the experimental data [1]. As for fluid flow with heating conditions, due to the decrease of dynamic viscosity with the increase of temperature near the wall region, the wall shear stress is decreased and the heat transfer coefficient is increased.

Two methods were used to take account of variable property effects on pressure drops and heat transfer coefficients of forced laminar flow in straight tubes. One method is to still use the constant property equations but the properties should be calculated at the effective reference temperature. Deissler [2] numerically investigated fully developed gas and liquid-metal laminar flow with variable properties and proposed a linear function to calculate the reference temperature, which was a function of T_w and T_b .

The other method which is widely used, is to correct the constant property assumption equations by using a property ratio correction factor. Sieder and Tate [3] measured the wall temperatures of oil laminar flow heated in straight tubes and proposed an equation to calculate the heat transfer coefficient with the property ratio correction factor of $(\mu_b/\mu_w)^{0.14}$. Herwig [4] analysed the property variation effects on pressure drops and heat transfer coefficients of laminar flow in straight tubes heated with low heat fluxes and deduced equations to calculate the friction factors and heat transfer coefficients.

To the authors' knowledge, there are few explicit equations to calculate friction factors and heat transfer coefficients of laminar convection with variable properties. The correction factors of the equations are not consistent. Furthermore, most existing equations are obtained by regression analysis of experimental data and cannot accurately reflect the property-temperature sensitivities at different fluid temperatures and sensitivities of different kinds of fluids. In this paper, the dynamic viscosity is approximated using first order Taylor series and explicit equations are obtained to calculate friction factors and heat transfer coefficients of forced liquid laminar convection heated in straight tubes.

NOMENCLATURE

Notation

f	[-]	friction factor
Nu	[-]	Nusselt number
q_w	[kW m^{-2}]	heat flux at the wall
r_0	[m]	tube radius
Re	[-]	Reynolds number
π	[-]	dimensionless parameter
$\pi_{S\mu T}$	[-]	$\pi_{S\mu T} = \left(2r_0 q_w \partial\mu/\partial T\|_b\right)/\left(\mu_b\lambda_b\right)$,
T	[K]	temperature
ΔT	[K]	temperature difference, $\Delta T = T_w - T_b$,
U	[m s^{-1}]	velocity magnitude in the axial direction

Greek letters

ε	[-]	deviation
λ	[W m^{-1} K^{-1}]	molecular thermal conductivity
μ	[kg s^{-1} m^{-1}]	dynamic viscosity
ρ	[kg m^{-3}]	density
τ	[Pa]	shear stress

Subscript

b	[-]	bulk
c	[-]	constant property
CFD	[-]	numerical results
l	[-]	local
m	[-]	area average
v	[-]	variable property
w	[-]	wall

CFD ANALYSIS

Heat transfer of forced laminar flow of water and ethanol with variable properties is simulated by Fluent software. The numerical results are used to investigate the liquid property variations in the radial direction and are used to verify the derived equations.

The governing equations of continuity, momentum and energy are solved by Fluent software with the finite volume method. The fluid properties are calculated by NIST package provided by Fluent. The coupling between velocity and pressure is resolved by SIMPLE algorithm. The convection terms are discretized by QUICK methods.

A schematic of the physical model and grids are shown in Fig. 1. No slip conditions and constant heat flux are imposed at the tube walls. The outlet boundary condition is pressure outlet (5MPa). The inlet boundary condition is mass flow inlet and the mass flux for every case is set to be 75kg/m^2-s. Uniform velocities and temperatures are set at the inlet. Laminar convection with constant properties at inlet temperature is also simulated to determine the entry length. The entry length is determined when the heat transfer coefficient variation in the axial direction $(\partial h/\partial z)$ is lower than 1%. The detailed boundary conditions are shown in Table 1. The radius is 2 mm.

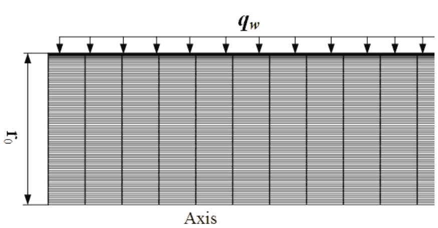

Figure 1 Schematic of the physical model and grids

Table 1 Boundary conditions

Cases	Liquid	Tube length (mm)	Inlet temperature (K)	Heat flux (kW/m^2)
1	water	1200	275	40
2	ethanol	2000	255	12
3	ethanol	2000	255	8

The grid independence is checked with meshes of different distributions. Case 1 is simulated with meshes of 50×600 (radial$\times$axial), 100×1200 and 200×2400 and the numerical results of friction factors and heat transfer coefficients are compared. The differences of numerical results with meshes of 100×1400 and 200×5000 are lower than 0.1%, which means the results with the mesh of 100×1400 is independent of grid.

The numerical models are validated by the friction factor and the Nusselt number for laminar flow with constant properties. In the fully developed flow regime, the friction factor deviations from the theoretical value of $64/\mathrm{Re}_b$ and the Nusselt number deviations from the theoretical value of 4.364 are both less than 1%.

EQUATION DEDUCTION

The property distributions in the radial direction of case 1 are shown in Fig. 2. The cross section is selected in the fully developed flow regime with $T_b=389.01K$ and $T_w=338.84K$. In Fig. 2, the physical properties are normalized by Eq. (1).

$$\phi=\phi_l/\phi_b \tag{1}$$

where ϕ_l means the local physical properties of densities, dynamic viscosities, thermal conductivities and specific heats and ϕ_b means the properties at T_b. Fig. 2 shows that the dynamic viscosity variations are much more dramatic than the variations of density, thermal conductivity and specific heat. Then the analysis of all property variation effects on pressure drops and heat transfer performances for water can be simplified to be the analysis of dynamic viscosity variation effects. Actually, many researchers [2, 3, 5] have concluded that for liquid convection, the variations of density, thermal conductivity and specific heat can be assumed invariant compared with the larger variations of dynamic viscosities.

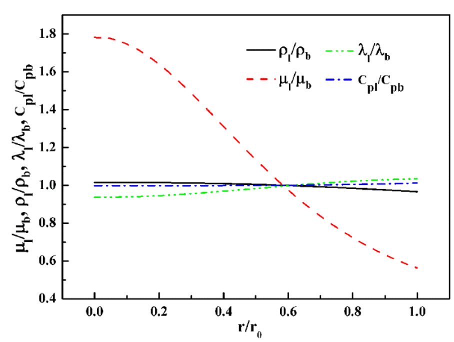

Figure 2 Normalized physical property distributions in the radial direction

According to researchers [2, 6], whether the properties are constant or variable, velocity distributions can be obtained by solving Eq. (2) and temperature distributions can be obtained by solving Eq. (3).

$$U=\int_{r_0}^{r}-\frac{\tau_w}{\mu r_0}rdr \tag{2}$$

$$T=T_w-\frac{2q_w}{U_m r_0}\int_r^{r_0}\frac{\int_0^r rUdr}{\lambda r}dr \tag{3}$$

For constant property assumptions, the velocity distribution calculated by Eq. (4) and temperature distribution calculated by Eq. (5) can be obtained by solving Eq. (2) and (3).

$$U=\frac{1}{2}\frac{\tau_w}{\mu_b r_0}\left(r_0^2-r^2\right) \tag{4}$$

$$T=T_w-\frac{4q_w r_0}{\lambda_b}\left[\frac{3}{16}-\frac{1}{4}\left(\frac{r}{r_0}\right)^2+\frac{1}{16}\left(\frac{r}{r_0}\right)^4\right] \tag{5}$$

However, for variable property assumption, Eq. (2) and (3) are too complicated to get theoretical solutions. Kays et al. [5] proposed to use the constant property temperature distribution to calculate the dynamic viscosity distribution. Then Eq. (2) and Eq. (3) are solved to get new velocity and temperature distributions. The new approximated temperature distribution will be used for further iterations. However, this method can only get the numerical results for specific conditions due to the complex viscosity-temperature function. In this paper, the function between the reciprocal of the dynamic viscosity and temperature is approximated using first order Taylor series and the reciprocal of dynamic viscosity distribution in the cross section is obtained using the constant property temperature distribution. With the first order approximation, explicit equations for the friction factors and the Nusselt number are obtained.

Liquid physical properties depend on pressures and temperatures. However, Hervig [4] has found that the physical properties depend much on temperatures than on pressures and the pressure effects on dynamic viscosity variations in the radial direction can be neglected. Setting the bulk temperature to be the reference state, the function between the reciprocal of dynamic viscosity and temperature can be approximated using the first order Taylor series.

$$\frac{1}{\mu}=\frac{1}{\mu_b}+(T-T_b)\frac{d}{dT}\left(\frac{1}{\mu}\right)\bigg|_b \tag{6}$$

With Eq. (6), the constant property temperature distribution shown in Eq. (5) is used to calculate the reciprocal of dynamic viscosity distribution. The reciprocal of dynamic viscosity distributions are given by Eq. (7).

$$\frac{1}{\mu}=\frac{1}{\mu_b}-\frac{4q_w r_0}{\lambda_b}\frac{d}{dT}\left(\frac{1}{\mu}\right)\bigg|_b\left\{\left[\frac{7}{96}-\frac{1}{4}\left(\frac{r}{r_0}\right)^2+\frac{1}{16}\left(\frac{r}{r_0}\right)^4\right]\right\} \tag{7}$$

Combine Eq. (2) and Eq. (7), the velocity distribution can be deduced as,

$$\begin{aligned}U=&\frac{1}{2}\frac{\tau_w r_0}{\mu_b}\left[1-\left(\frac{r}{r_0}\right)^2\right]+\\ &\frac{4q_w r_0}{\lambda_b}\tau_w r_0\frac{d}{dT}\left(\frac{1}{\mu}\right)\bigg|_b\left[\frac{1}{96}\left(\frac{r}{r_0}\right)^6-\frac{1}{16}\left(\frac{r}{r_0}\right)^4+\frac{7}{192}\left(\frac{r}{r_0}\right)^2+\frac{1}{64}\right]\end{aligned} \tag{8}$$

With Eq. (9), the relationship between the averaged velocity magnitude and the wall shear stress can be expressed as Eq. (10).

$$U_m=\frac{\int_0^{r_0}2\pi rUdr}{\pi r_0^2} \tag{9}$$

$$U_m=\frac{\tau_w r_0}{4\mu_b}+\frac{d}{dT}\left(\frac{1}{\mu}\right)\bigg|_b\frac{q_w r_0}{16\lambda_b}\tau_w r_0 \tag{10}$$

Combine Eq. (3) and Eq. (8), the temperature distribution can be obtained as Eq. (11).

$$\begin{aligned}T=&T_w-\frac{q_w r_0}{\lambda_b}\frac{\tau_w r_0}{\mu_b U_m}\left[\frac{3}{16}-\frac{1}{4}\left(\frac{r}{r_0}\right)^2+\frac{1}{16}\left(\frac{r}{r_0}\right)^4\right]\\ &-\left(\frac{q_w r_0}{\lambda_b}\right)^2\frac{\tau_w r_0}{U_m}\frac{d}{dT}\left(\frac{1}{\mu}\right)\bigg|_b\left[\begin{array}{l}\frac{85}{2304}-\frac{1}{32}\left(\frac{r}{r_0}\right)^2-\\ \frac{7}{384}\left(\frac{r}{r_0}\right)^4+\frac{1}{72}\left(\frac{r}{r_0}\right)^6\\ -\frac{1}{768}\left(\frac{r}{r_0}\right)^8\end{array}\right]\end{aligned} \tag{11}$$

Combine Eq. (11) and Eq. (12), the bulk temperature can be expressed by Eq. (13),

$$T_b=\frac{\int_0^{r_0}2\pi r\rho UTdr}{\rho U_m\pi r_0^2} \tag{12}$$

$$\begin{aligned}T_b=&T_w-\frac{11}{24}\left(\frac{f_v\mathrm{Re}}{64}\right)^2\frac{q_w r_0}{\lambda_b}\\ &-\frac{19}{96}\left(\frac{f_v\mathrm{Re}}{64}\right)^2\left(\frac{q_w r_0}{\lambda_b}\right)^2\mu_b\frac{d}{dT}\left(\frac{1}{\mu}\right)\bigg|_b\\ &-\frac{1405}{64512}\left(\frac{f\,\mathrm{Re}}{64}\right)^2\left(\frac{q_w r_0}{\lambda_b}\right)^3\left(\mu_b\frac{d}{dT}\left(\frac{1}{\mu}\right)\bigg|_b\right)^2\end{aligned} \tag{13}$$

According to Eq. (10), the Darcy friction factor for variable properties can be deduced as:

$$f_v=\frac{64}{\mathrm{Re}_b}\frac{1}{\left(1+\frac{d}{dT}\left(\frac{1}{\mu}\right)\Big|_b\mu_b q_w r_0\Big/4\lambda_b\right)} \tag{14}$$

According to Eq. (13), the Nusselt number can be deduced as,

$$Nu_v=\frac{1}{\left(f_v\mathrm{Re}_b/64\right)^2\left\{\begin{array}{l}\left(\frac{11}{48}\right)+\left(\frac{19}{48}\right)\left(\frac{r_0q_w\mu_b}{4\lambda_b}\frac{d}{dT}\left(\frac{1}{\mu}\right)\Big|_b\right)+\\ \left(\frac{1045}{8064}\right)\left(\frac{r_0q_w\mu_b}{4\lambda_b}\frac{d}{dT}\left(\frac{1}{\mu}\right)\Big|_b\right)^2\end{array}\right\}} \tag{15}$$

RESULTS AND DISCUSSION

Temperature effects on liquid viscosity variations have been widely investigated [7-10]. In this paper, forced laminar convections of water and ethanol are investigated to verify the deduced equations. In reference [11], Eq. (16) is used to calculate dynamic viscosities of ethanol and water. Then, $d(1/\mu)/dT\big|_b$ can be calculated by Eq. (17).

$$\frac{1}{\mu}=1000e^{-\left(A+B/T+CT+DT^2\right)} \tag{16}$$

$$\frac{d}{dT}\left(\frac{1}{\mu}\right)\bigg|_b=\frac{1}{\mu_b}\left(B/T_b^2-C-2DT_b\right) \tag{17}$$

where A, B, C and D are constants and are shown in Table 2.

Table 2 Constants for Eq. (16)

Liquids	A	B	C	D
water	-24.71	4209	0.04527	-3.376E-5
ethanol	-6.21	1614	0.00618	-1.132E-5

Velocity distributions in the cross section calculated by the deduced equation (Eq. (8)) and distributions calculated by the constant property assumption equation (Eq. (4)) are compared with the numerical results. Velocity distributions of case 1 (water, ΔT=50.18 K and $T_b = 338.84\,K$) are shown in Fig. 3, distributions of case 2 (ethanol, ΔT=62.31 K, $T_b = 350.31\,K$) are shown in Fig. 4. Figures 3 and 4 show that, when ΔT is higher than 50 K, the velocities calculated by the constant property assumption equations are much lower than the numerical results, while the deduced equations agree well with the numerical results.

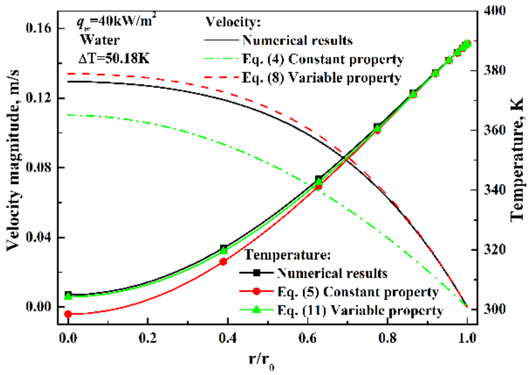

Figure 3 Velocity and temperature distribution in the cross section of case 1 (water)

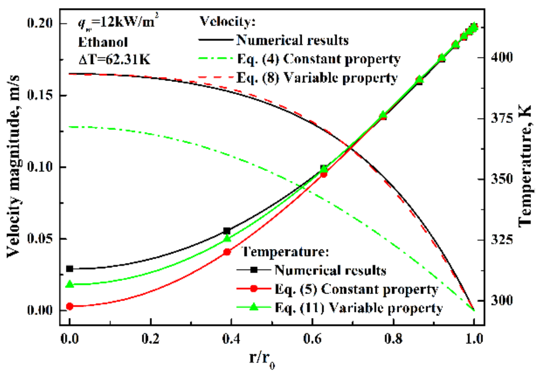

Figure 4 Velocity and temperature distribution in the cross section of case 2 (ethanol)

Temperature distributions in the cross section calculated by the present deduced equation (Eq. (11)) and distributions calculated by the constant property assumption equation (Eq. (5)) are compared with the numerical results. Temperature distributions of case 1 are shown in Fig. 3, distributions of case 2 are shown in Fig. 4. Figures 3 and 4 show that the temperatures calculated by the constant property assumption equations are much lower than the numerical results. Near the axial region, the temperatures calculated by the deduced equation are lower than the numerical results. However, the deduced equation shows better predictions than the constant property equation. Comparing with the velocity deviations of Eq. (4) from numerical results, the temperature deviations of Eq. (5) are much lower. Because the dynamic viscosity effects on velocity distributions are direct while the effects on temperature distributions are indirect [12]. The variable dynamic viscosities first distort the velocity distribution, then the temperature distributions are influenced by the distorted velocity distributions.

Friction factors calculated by the deduced equation (Eq. (14)) and friction factor calculated by the constant property assumption (Eq. (18)) are compared with numerical results. Friction factor versus bulk temperature variations of case 1 (water) are shown in Fig. 5 and variations of case 2 (ethanol) are shown in Fig. 6. Figures 5 and 6 show that friction factors predicted by the constant property assumption equation are much higher than the numerical results, while the deduced equations show good prediction. In Fig. 5, the maximum deviation of Eq. (18) is 44.05% while the maximum deviation of Eq. (14) is 4.17%. In Fig. 6, the maximum deviation of Eq. (18) is 67.68% while the maximum deviation of Eq. (14) is 1.14%. Figures 5 and 6 show that the deviations of the constant property assumption equation from the numerical results decrease with the increase of bulk temperature, which is caused by the decreasing of $d(1/\mu)/dT$ with the increasing of bulk temperatures.

$$f_c = 64/\mathrm{Re}_b \tag{18}$$

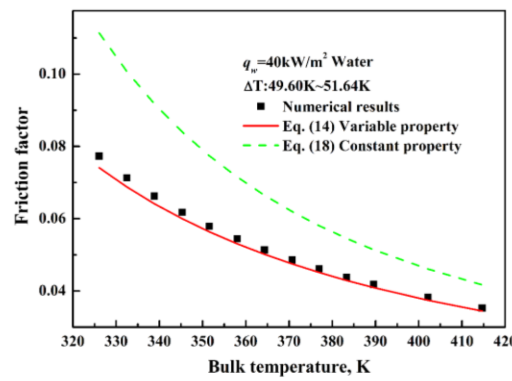

Figure 5 Friction factor versus bulk temperature variations of case 1 (water)

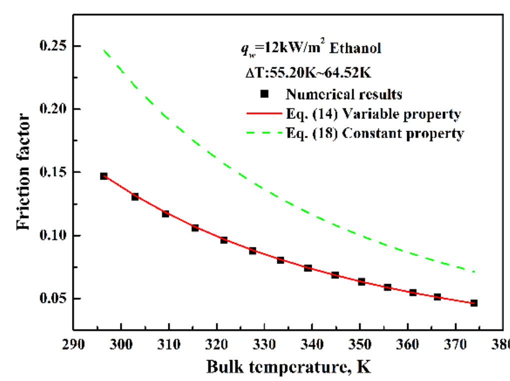

Figure 6 Friction factor versus bulk temperature variations of case 2 (ethanol)

Nusselt numbers calculated by the deduced equation (Eq.(15)) and Nusselt numbers calculated by the constant property assumption equation (Eq. (20)) are compared with numerical results. The deviations of Eq. (20) from the numerical results, ε_c , and deviations of Eq. (15), ε_v , are defined by Eq. (19),

$$\varepsilon_c = \left|\frac{Nu_{CFD} - Nu_c}{Nu_{CFD}}\right| \quad \varepsilon_v = \left|\frac{Nu_{CFD} - Nu_v}{Nu_{CFD}}\right| \tag{19}$$

where Nu_{CFD} is the numerical result. The deviations of case 1 (water) are shown in Table 3 and deviations of case 2 (ethanol) are shown in Table 4. Tables 3 and 4 show that Nusselt numbers predicted by the constant property assumption equations are lower than numerical results while the deduced equations show good predictions. For case 1 (water), the maximum deviation of Eq. (20) is 12.17% while the maximum deviation of Eq. (15) is 1.95%. For case 2 (ethanol), the maximum deviation of Eq. (20) is 16.69% while the maximum deviation of Eq. (15) is 1.09%. Tables 3 and 4 show that the deviations of constant property assumption equation decrease with the increase of bulk temperatures, which is caused by the decrease of $d(1/\mu)/dT$ with the increase of bulk temperatures. The Nusselt number deviations of the constant property assumption equation are much lower than the friction factor deviations. Because the dynamic viscosity effects on velocity distributions are direct while the effects on temperature distributions are indirect [12].

$$Nu_c = \frac{48}{11} \tag{20}$$

Table 3 Nusselt number versus bulk temperature variations of case 1 (water)

T_b	ΔT	Nu_{CFD}	ε_c	ε_v
326.07	49.60	4.97	12.17%	1.38%
351.58	50.45	4.72	7.61%	1.09%
364.30	50.62	4.66	6.36%	1.43%
389.61	50.99	4.58	4.65%	1.68%
414.68	51.64	4.52	3.37%	1.95%

Table 4 Nusselt number versus bulk temperature variations of case 2 (ethanol)

T_b	ΔT	Nu_{CFD}	ε_c	ε_v
302.88	56.52	5.09	16.69%	1.09%
315.45	58.50	5.00	14.64%	0.19%
327.53	59.99	4.96	13.59%	0.71%
350.31	62.31	4.92	12.73%	0.86%
371.42	64.28	4.91	12.46%	0.71%

Figures 5 and 6 show that the deviations of the constant property assumption equations from the numerical results decrease with the increase of bulk temperature, this is caused by the decrease of viscosity temperature sensitivity with the increase of temperature. With the decrease of the viscosity temperature sensitivities, the distortions of the velocity profile decrease. Kumar and Mahulikar [13] defined a dimensionless parameter of $\pi_{S\mu T}$ to evaluate the viscosity temperature sensitivity.

Comparing Eq. (18) with Eq. (14), the friction factor deviations between friction factors calculated by the constant property assumption equation and factors calculated by the deduced equation can be expressed by Eq. (21). Comparing Eq. (20) with Eq. (15), the Nusselt number deviations can be expressed by Eq. (22).

$$\varepsilon_f = \left|\frac{f_c - f_v}{f_v}\right| = \left|\frac{q_w r_0 \mu_b}{4_b \lambda_b}\frac{d}{dT}\left(\frac{1}{\mu}\right)\bigg|_b\right| = |\pi| \tag{21}$$

$$\varepsilon_{Nu} = \left|\frac{Nu_v - Nu_c}{Nu_v}\right| = \left|\frac{3\pi/11 + 73\pi^2/168}{(1+\pi)^2}\right| \tag{22}$$

Eq. (21) shows that the friction factor deviations decrease with the decrease of $|\pi|$. Calculate $d\varepsilon_{Nu}/d\pi$ with Eq. (22), we can find that when π is larger than -0.45, ε_{Nu} increase with the increase of $|\pi|$. The physical value of π is always larger than -0.45, so ε_{Nu} always increase with the increase of $|\pi|$.

Due to the decreasing of $d(1/\mu)/dT$ with the increasing temperature, $|\pi|$ decreases with the increasing of bulk temperature. Then the friction factor deviations and the Nusselt number deviations decrease with the increase of bulk temperature, as shown in Figures 5 and 6 and Tables 3 and 4. When the properties are assumed to be constant, $|\pi|$ will be zero, the deduced equations will regressed to be the constant property assumption equations.

$|\pi|$ increases with the increasing of heat flux. Laminar convection of ethanol with heat flux of 8kW/m^2 (case 3) is simulated and the results are used to evaluate the heat flux effects. The friction factor variations of case 2 and case 3 are shown in Fig. 7. Fig. 7 shows that the friction factor deviations of the constant property assumption equations increase with the increase of heat flux.

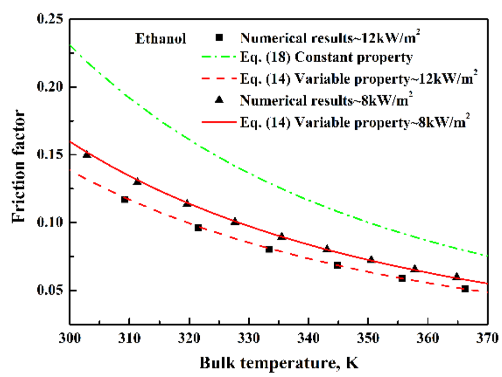

Figure 7 Friction factor versus bulk temperature of case 2 (12kW/m^2) and case 3 (8kW/m^2)

Divide Eq. (22) by Eq. (21), the ratio, $\varepsilon_f/\varepsilon_{Nu}$ can be deduced as,

$$\frac{\varepsilon_f}{\varepsilon_{Nu}} = \frac{(1+\pi)^2|\pi|}{\left|\frac{3}{11}\pi + \frac{73}{168}\pi^2\right|} \tag{23}$$

when π is larger than -0.45, the minimum value of $\varepsilon_f/\varepsilon_{Nu}$ is larger than 3.43. That is why the friction factor deviations of the constant property assumptions are larger than Nusselt number deviations.

CONCLUSION

The existing equations for friction factors and heat transfer coefficients of forced laminar convection with variable fluid properties are obtained by regression analysis of experimental data with a specific kind of fluid. Furthermore, they cannot reflect the property-temperature sensitivities at different fluid temperatures and sensitivities of different kinds of fluids. The correction factors of these equations are also not consistent. In this paper, the function between the reciprocal of dynamic viscosity and temperature is approximated using first order Taylor series. Equations for friction factors and heat transfer coefficients of forced liquid laminar flow without entry effects are obtained based on the approximation. Heat transfer of laminar flow of water and ethanol in straight tubes with constant heat flux are simulated to validate the deduced equations. The main conclusions are:

(1) The dynamic viscosity variations in the cross section are much larger than the variations of thermal conductivity, density and specific heat. Based on a modified reciprocal of dynamic viscosity distribution in the cross section, new explicit friction factor and heat transfer coefficient equations of forced liquid laminar convection are obtained.
(2) The deduced equations show better predictions of friction factors and Nusselt numbers for different kinds of fluids and at different bulk temperatures.
(3) A dimensionless parameter of $|\pi|$ is defined to evaluate the dynamic viscosity variation effects on pressure drops and heat transfer coefficients. The physical property variation effects increase with the decrease of $|\pi|$, which means the variation effects increase with the decreasing of bulk temperature and with the increasing of heat flux.

REFERENCES

[1] G. Poots, G.F. Raggett, Theoretical results for vairiable property laminar boundary layers in water, International Journal of Heat and Mass Transfer, 10 (1967) 597-610.
[2] R.G. Deissler, Analytical investigation of fully developed laminar flow in tubes with heat transfer with fluid properties variable along the radius, in, NACA, Washington, 1951.
[3] E.N. Sieder, G.E. Tate, Heat transfer and pressure drop of liquids in tubes, Industrial and Engineering Chemistry, 28 (1936) 1429-1435.
[4] H. Herwig, The effect of variable properties on momentum and heat transfer in a tube with constant heat flux across the wall, International Journal of Heat and Mass Transfer, 28 (1985) 423-431.
[5] W.M. Kays, M.E. Crawford, B. Weigand, Convective heat and mass transfer, Tata McGraw-Hill Education, New York, 2012.
[6] B.S. Petukhov, Heat transfer and friction in turbulent pipe flow with variable physical properties, Advances in Heat Transfer, 6 (1970) 503-564.
[7] E. Goletz, D. Tassios, An antoine type equation for liquid viscosity dependency to temperature, Industrial and Engineering Chemistry Process Design and Development, 16 (1977) 75-79.
[8] D.V. Velzen, R.L. Cardozo, H. Langenkamp, Liquid viscosity and chemical constitution of organic compounds: a new correlation and a compilation of literature data, Commission of the European Communities, Ispra, 1972.
[9] C.L. Yaws, J.W. Miller, P.N. Shah, C.L. Yaws, G.R. Schorr, P.M. Patel, Physical and thermodynamic properties 24 correlation constants for chemical compounds, Chemical Engineering, 83 (1976) 153-162.
[10] C.R. Duhne, Viscosity temperature correlations for liquids, Chemical Engineering, 86 (1979) 83-91.
[11] R.C. Reid, J.M. Prausnitz, B.E. Poling, The properties of gases and liquids, McGraw-Hill, New York, 1987.
[12] S.P. Mahulikar, H. Herwig, Physical effects in laminar microconvection due to variations in incompressible fluid properties, Physics of Fluids, 18 (2006) 073601-073612.
[13] R. Kumar, S.P. Mahulikar, Effect of temperature-dependent viscosity variation on fully developed laminar microconvective flow, International Journal of Thermal Sciences, 98 (2015) 179-191.